A Virtual Reality based 3D Real-Time Interactive Brachytherapy Simulation of Needle Insertion and Seed Implantation

Xiaogang Wang and Aaron Fenster

Robarts Research Institute, 100 Perth Drive, London, ON, N6A 5K8 Canada
Email: xwang@imaging.robarts.ca

ABSTRACT

Virtual reality based simulation can facilitate training, rehearsal, and intra-operative assistance used to improve the accuracy and quality of prostate brachytherapy. In this paper, we introduce a 3D real-time interactive simulation of needle insertion and seed implantation for prostate brachytherapy and report on the haptic feedback model used in this system. A deformable soft tissue model has been generated based on the restricted 3D ChainMail method to account for tissue deformation during needle insertion. A direct manipulation model for dynamic needle-tissue interaction was adopted. Haptic feedback, mimicking forces experienced in real procedures was provided to enhance realism and training outcome. The brachytherapy procedure has been simulated to demonstrate the errors caused by tissue deformation. Functionally, the simulation software is divided into two parts: visual simulation and haptic rendering. The preliminary implementation results of this simulation have demonstrated to be useful and promising.

1. INTRODUCTION

By using real-time TRansrectal UltraSound (TRUS) guided brachytherapy, radioactive seeds are implanted into the prostate according to a pre-computed dose plan. This technique is useful for treating early stage prostate cancer due to fewer complication, faster recovery, and shorter hospital stay. The procedure's success depends on accurate seed delivery matching the dosimetric plan so as to maximize the destruction of the cancerous cells while minimizing healthy tissue damage. However, when a needle is inserted into the prostate, the needle and the tissue interact resulting in soft tissue deformation. As a result, physicians must learn to compensate as well as be well trained. By facilitating training, rehearsal, and intra-operative assistance, a virtual reality based brachytherapy simulation could improve the accuracy and quality of prostate brachytherapy.

Virtual reality based surgical simulations, bringing both visual and tactile sensations to its users require dynamic response from realistic tissue and surgical tool modeling. The challenges include physical realistic modeling, tradeoffs among physical and visual realism, cost and the demands of real-time interaction.

Simulations of needle insertion for training purposes have been implemented earlier by Brett et. al. [1], who constructed a mechanical surgical needle resistance force simulation. By using a computer related technique, Kimura et. al. [2] presented a prostate brachytherapy training rehearsal system incorporating 3D visualization of the body and haptic feedback. Their system includes a realistic virtual environment of organs surrounding the prostate and needle deflection during insertion; however, they did not take into account soft tissue deformation. DiMaio and Salcudean in their pioneering work [3] presented a 2D real-time needle insertion simulation, which used a quasi-static *Finite Element Method* (FEM) for soft tissue deformation based on their experimentally estimated needle shaft force modeling. In their approach, they achieved 500Hz haptic feedback update rate and high displacement accuracy. In another 2D prostate brachytherapy simulation, Alterovitz et. al. [4] used a dynamic FEM formulation for soft tissue deformation computation for accurate surgical planning with needle insertion and seed implantation. Nienhuys and Stappen [5] proposed another FEM solution for 3D needle insertion simulation with non-linear material modeling using an iterative algorithm. To the best of our knowledge, no 3D real-time interactive needle insertion simulations have been reported.

In this paper, we introduce a 3D real-time interactive simulation of needle insertion and seed implantation for prostate brachytherapy and report on our haptic feedback method. Our goal is to achieve a complete 3D real-time simulation with a realistic tissue deformation and haptic feedback for augmented training and intra-operative assistance. To perform 3D real-time interactive simulation, we used the restricted 3D ChainMail model [6, 7, 13]. A direct manipulation model for needle-tissue interaction was adopted. Four brachytherapy steps have been simulated. The preliminary implementation results of this simulation demonstrated to be useful and promising.

2. SYSTEM AND METHODS

2.1 System Description

Figure 1 outlines the components of the system. The online real-time simulation involves interactive visual simulation, haptic feedback, and TCP/IP based communication. Our soft tissue prostate volumetric model was based on a segmented 3D US image of the prostate obtained priori to brachytherapy [8]. The 3D ChainMail prostate surface model was reconstructed and used to allow visual rendering and be suitable for ChainMail deformation computation. All ChainMail tissue model parameters are adjustable with a user dialog interface. The visual simulation module runs in two cycles: one is at 30Hz for graphical model rendering and another is at 200Hz for performing soft tissue deformation computation as well as user interaction. The haptic module is executed at 1kHz. Both parts communicate with each other in a client-server manner. A 6-DoF Phantom™ (Premium 1.5, SensAble) was used to provide force feedback and needle control. The simulation runs on a single 2.1 GHz PC computer, which acts as both server and client, though a distributed architecture has already been adopted.

2.2 Computing Soft Tissue Deformations

A. 3D ChainMail method

In the 3D ChainMail algorithm [6], volume elements were linked to their 6 nearest neighbors (front, back, right, left, top,

and bottom). When one element is moved beyond its limits, which defines a geometric constrain zone, neighboring links absorb the movement by taking up slack in the structure. Figure 2 shows the 1D case of the ChainMail model. In a similar way, the 2D and 3D ChainMail model can be described (see [6, 7] for details).

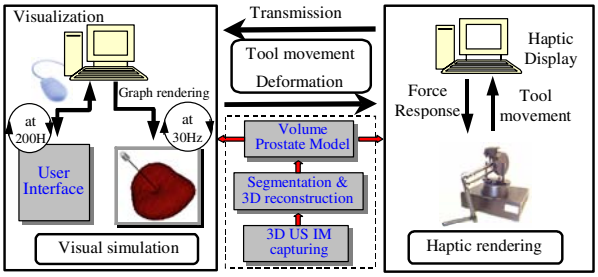

Fig. 1 Diagram of system structure of the prostate brachytherapy simulation. It includes 3 components: the left solid box is the visual simulation module that performs all computations required for simulating soft tissue deformation, needle motion and graphic rendering; the right solid box is the haptic rendering module consisting of haptic display and user input; and the centered dashed box supplies the prostate model.

A set of geometric constrains that consists of two pairs of translations and 2 single shears (assuming different in x and y) in the 2D case (Fig. 3) are used to denote material properties. These constraints are used to represent elastic, viscoelastic, plastic, and rigid materials. With defined geometric constraints, particularly for 3D objects, the ChainMail model can be used to simulate the deformation of soft tissue.

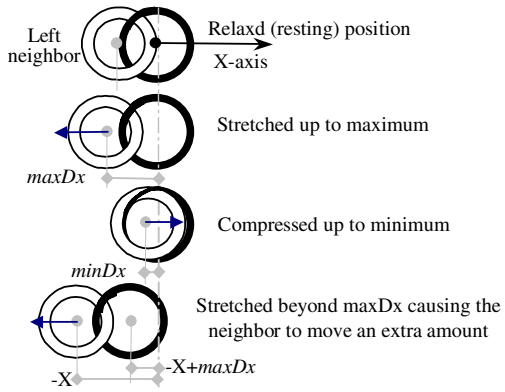

Fig.2 1D chain model of two chain elements.

B. *Restricted 3D ChainMail method*

With the original definition of shearing constraints in the ChainMail model, certain deformation could lead to geometric shape degradation or even "self-interference". In these cases, the geometric topology structure can be destroyed or changed resulting in inconsistent geometries [13]. This is caused by unrestricted or unreasonable designation of shearing constraints. The original shearing constraints were defined such that they didn't take into account rotational fiducials with respect to which shearing is calculated. However, the shearing at different distances with respect to rotational fiducials only obeys angle constraints. The magnitude of shearing displacement is usually proportional to the distance for a linear elastic material.

In order to overcome this deficiency, we propose a restricted ChainMail method (this name is dubbed because of a restricted shearing constraint) [13]. We therefore define the shearing limits as angle constraints, *maxHoriRx* and *maxVertRy* (Fig. 4). Moreover, a necessary and sufficient condition of self-interference free of geometric constraints is exploited as:

$$maxHoriRx + maxVertRy < 90^0 \quad (1)$$

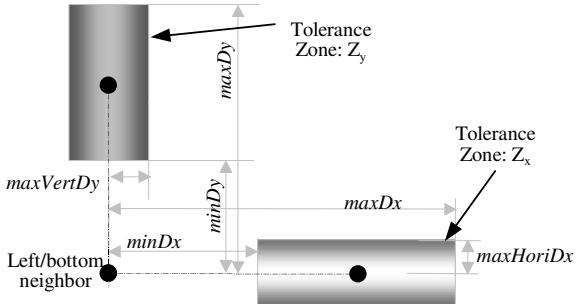

Fig. 3 Geometric constraints of the 2D chain model

Accordingly, the actual shearing displacements are:

$$maxHoriSx = maxDx * tan(maxHoriRx) \quad (2)$$

and a similar equation applies to *maxVertSy*.

The geometric topology of ChainMail model can be preserved in all circumstance with a defined trapezium of "tolerance zone" only if equation (1) is satisfied. Extension of the new shearing constraints from 2D ChainMail to 3D ChainMail is straightforward. The 2D trapezium is replaced by 3D frustum of "tolerance zone".

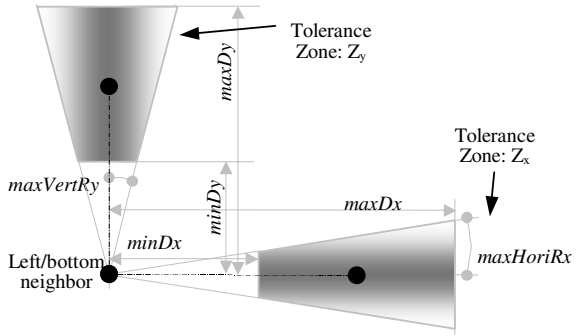

Fig.4 Geometric constraints of restricted 2D chain model

C. *Tissue Deformation Computation*

The 3D restricted ChainMail method can meet the requirement of real-time simulation in performing soft tissue deformation computation. In this simulation, the prostate model, obtained from a segmented 3D US prostate image (323x187x176), consists of 19304 elements and 2999 surface elements, generating 6397 surface triangles. The number of ChainMail model elements here is approximately 1/9 of all voxels, which resulted from a process of turning an anisotropic volume representation (the voxel size in x, y directions is 1/3 of that in z) to an isotropic representation (cubic voxel). Note that it is not necessary to use all the voxels in the soft tissue model for deformation computation (although this was advocated in [7]) as this could lead to an expensive computation. Given a large displacement with respect to the deformation constraint (so that all elements will be moved), the timing of the 3D ChainMail "searching-absorbing" algorithm for displacing-neighbours is less than 4ms. Because of the locality of the deformation, however, the actual time required for calculating deformation in each cycle is even further reduced. In our simulation, tissue homogeneity has been assumed so we used a set of uniform geometric constraints:

$$maxDx = maxDy = maxDz = 1.75 \text{ vox.} \quad (3)$$

$$minDx = minDy = minDz = 0.55 \text{ vox.} \quad (4)$$

$$maxHoriRx = maxVertRy \leq \arctan(1/2) \quad (5)$$

The result has provided an adequate realistic effect.

2.3 Direct Needle-Tissue Interaction

The *displacement-based* descriptive methods [9,10] require that the desired displacement be explicitly and directly applied to the object when instrument-tissue interaction takes place. Thus, for descriptive methods, one must design a strategy that bridges the instrument's movement and tissue deformation, rather than using external force-driven in physically based methods.

In order to enhance the simulation realism, we adopt a direct manipulation strategy based on the following criteria:

a) Simple and fast, to meet real-time computation requirement;
b) Direct or indirect relationship to physical laws to better approximate reality; and,
c) Easy to adjust parameters to optimize the model's behaviour.

In our current implementation, we assume that the needle is rigid and no deflection occurs. We also assume that only the needle tip triggers the tissue movement and the relative motion between needle and tissue complies with the "stick-slip" mode that has been similarly used in other systems [3, 4].

Ensuring that the model can be related to appropriate physical kinetic properties and associated "external forces" [11], we implemented a non-linear Gaussian transmission function to approximate the interaction between the moving needle and soft tissue elements as follows:

$$\Delta_{sel} = \begin{cases} \Delta_{tip}, & \text{if } u_{tip} < u_{cri} \text{ and } \vec{V}_{tip} \bullet \vec{r} > 0; \\ \Delta_{tip} \exp\{-[K_V^{-1}(|\vec{V}_{tip}| - |\vec{V}_0|)^2 U(|\vec{V}_{tip}| - |\vec{V}_0|) \\ \quad + K_S^{-1}(u_{tip} - u_{cri})^2]\}, & \text{if } u_{tip} \geq u_{cri} \text{ and } \vec{V}_{tip} \bullet \vec{r} > 0; \\ K_{ret}^{-1}\Delta_{tip}, & \text{if } \vec{V}_{tip} \bullet \vec{r} < 0. \end{cases} \quad (6)$$

$$\vec{V}_{tip} = \frac{d\vec{u}_{tip}}{dt} \quad (7)$$

where Δ_{tip} and Δ_{sel} are step-lengths for movement of the needle tip and for a "selected" element of soft tissue connected to the needle tip at each loop respectively; u_{cri} represents the critical puncture depth at which the needle will puncture the membrane; u_{tip} is the insertion depth; $\vec{V}_{tip}$ and $\vec{V}_0$ denote relative speeds ($\vec{V}_0$ is the critical static-frictional constant speed) of the needle tip; $U(\cdot)$ is the unit step function; K_V and K_S are estimated coefficients relevant to the speed of the needle and insertion depth respectively; K_{ret} is a coefficient relevant to the needle retraction; and $\vec{r}$ is the directional vector pointing to the needle's destination.

Three phases of the needle-tissue interaction, i.e., membrane contraction ($u_{tip} < u_{cri}$ and $\vec{V}_{tip} \bullet \vec{r} > 0$), needle penetration ($u_{tip} > u_{cri}$ and $\vec{V}_{tip} \bullet \vec{r} > 0$), and retraction ($\vec{V}_{tip} \bullet \vec{r} < 0$), have been taken into consideration in the equation (6).

3. HAPTIC FEEDBACK MODEL

A networking-based interactive haptic-rendering subsystem with a force computational model has been developed and integrated into the visual simulation for enhancing the simulation with the use of a haptic display. A 6-DoF Phantom™ is used to provide the user with force feedback when simulating needle insertion.

For haptic feedback, a force is calculated according to the approach described in [12]:

$$F = F_R + F_C + F_G \quad (8)$$

where F represents the total effect of forces exerted to the operator; F_G is the force to compensate for gravity; F_C is the force that constrains the needle along the direction of a straight-line movement plus resistive forces that are generated by damping effects and friction; and F_R is the force required to penetrate the tissue surface.

Considering the two parts of F_C, we have

$$F_C = \underbrace{K \cdot K_C \cdot \vec{S}_{offset}}_{\text{part 1}} + \underbrace{K_V \cdot \vec{V}_{tip} + K_f \cdot \vec{u}_{tip}}_{\text{part 2}} \quad (9)$$

and

$$\vec{S}_{offset} = \text{Vector}(P_{tip} - P_{proj} \mid \vec{L}_{path}),$$

$$\vec{L}_{path} = \text{Vector}(P_{punc} - P_{prev})$$

where $\vec{S}_{offset}$ is the offset of the needle tip from its straight-line path; P_{tip} is the current position of needle tip; $P_{proj} \mid \vec{L}_{path}$ is the projection of the current position of the needle tip on the insertion path; P_{prev} is the immediate previous position of the needle tip; P_{punc} is the entry point of the needle on the surface of prostate; and $\vec{L}_{path}$ is the insertion path directional vector.

Also, we have

$$F_R = \begin{cases} \text{constant}, & \text{if } u_{tip} = u_{cri}; \\ 0, & \text{otherwise.} \end{cases} \quad (10)$$

The same graphical model of the prostate was used in the haptic virtual world. Several functional sub-modules associated with the force computational model have been implemented: user interaction in 3D workspace, assignment of mechanical properties, and context-based interpretation of user input.

At present, haptic feedback is uncoupled from visual deformation. Later we will couple haptic rendering to visual deformation. In addition, a prostate's anatomical environment (*rectal wall*, *fat*, and *prostate capsule/gland*) will be provided to increase the realism.

4. IMPLEMENTATION RESULTS

The brachytherapy procedure has been simulated to demonstrate the errors caused by soft tissue deformation. Figure 5 depicts a screen snapshot of the software interface of our simulation system. Figure 6 illustrates four steps of the procedure: (1) specification of seed positions inside the prostate (6(a)); (2) placement of a needle according to a specified entry point and trajectory (6(b)). A landmark denotes the entry point and a thick and dashed line denotes the needle insertion trajectory; (3) insertion of the needle into the prostate consisting of two sub-steps: membrane contraction (6(c)) and penetration insertion (6(d)); and, (4) retraction of the needle after seed implantation (6(e)). In Fig. 6 (f) and (g), inaccurate placement of the seeds results in imperfect dose coverage of the prostate. Clearly this type of error can be compensated for if proper preplanning is adopted (not discussed here).

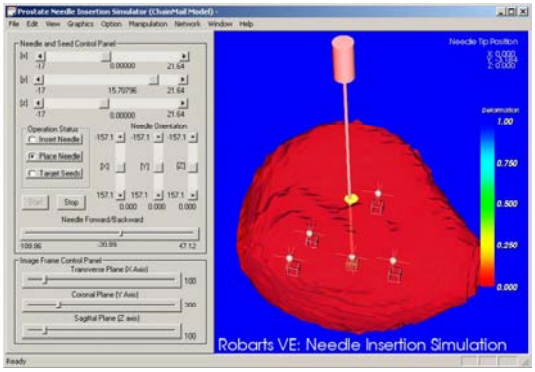

Fig. 5 A screen snapshot of 3D prostate brachytherapy simulation

The preliminary validation was based on an expert's examination by comparing simulation results with two 3D TRUS images that were recorded before needle insertion and immediately after. No large errors on the surface deformation have been observed.

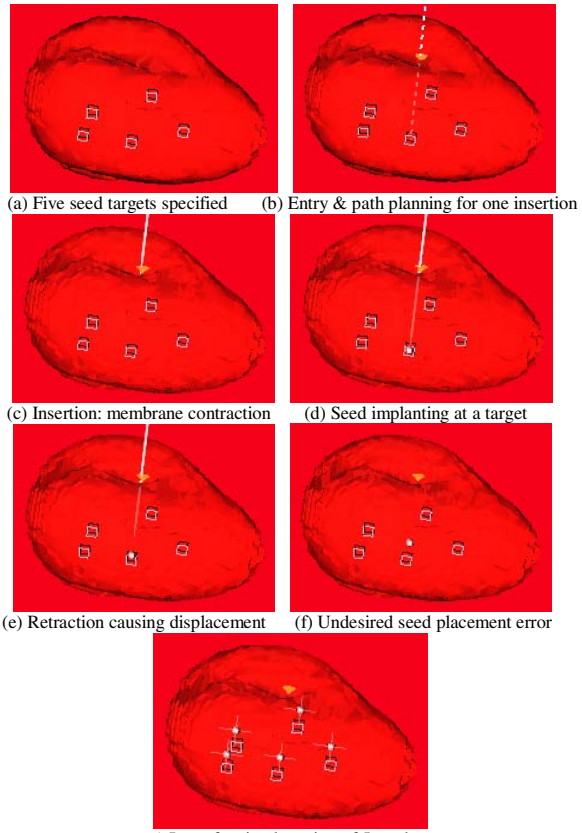

(a) Five seed targets specified (b) Entry & path planning for one insertion

(c) Insertion: membrane contraction (d) Seed implanting at a target

(e) Retraction causing displacement (f) Undesired seed placement error

g) Imperfect implantation of 5 seeds

Fig. 6 Simulation of delivery of 5 seeds to their targets with undesired errors. This 3D interactive simulation provides an environment for training and rehearsal of prostate brachytherapy.

5. CONCLUSION AND FUTURE WORK

We have developed a 3D real-time needle insertion simulation system for prostate brachytherapy. In this simulation, a prostate model was obtained from a segmented 3D US prostate image. Four key steps of prostate brachytherapy have been simulated. The 3D ChainMail based soft tissue deformation model, a direct manipulation model for needle-tissue interaction, and a haptic feedback module have been developed. The preliminary simulation results are promising and must be further tested.

Existing real-time interactive needle insertion simulations reported are mainly 2-D, limiting their utility. Our 3D simulation of prostate brachytherapy can overcome some of those limitations. In the future, the complexity of the prostate interior characteristics, such inhomogeneity and anisotropy, will be studied.

ACKNOWLEDGMENT

We thank Hanif Ladak for suggesting the use of the ChainMail model. A. Fenster holds a Canada Research Chair (Tier 1) in Biomedical Engineering. We acknowledge the support of the Canada Research Chair Program and support of CIHR and NSERC.

REFERENCES

[1] P. N. Brett, T. J. Parker, J. Harrison, T. A. Thomas, and A. Carr, Simulation of resistance forces acting on surgical needles, *Journal of Engineering in Medicine,* **211**, 335-347, 1997.

[2] A. Kimura, J. Camp, R. Robb, and B. Davis, A Prostate brachytherapy training rehearsal system – simulation of deformable needle insertion, *Medical Image Computing and Computer Assisted Intervention* (*MICCAI'*2002), 264-271.

[3] S. P. DiMaio and S. E. Salcudean, Needle insertion modeling simulation, *IEEE Trans. on Robotics and Auto*., **19**, 864-875, 2003.

[4] R. Alterovitz, J. Pouliot, R. Taschereau, I.C. Hsu, and K. Goldberg, Needle insertion and radioactive seed implantation in human tissues: simulation and sensitivity analysis, in *Proc. of the IEEE Int. Conf. on Robotics and Auto.*, Sept., 2003.

[5] H. Nienhuys and A. F. Stappen, Interactive needle insertions in 3D nonlinear material, Technical report, UU-CS-2003-019, 2003.

[6] S. F. F. Gibson, 3D ChainMail: a fast algorithm for deforming volumetric objects, in *Proc. of Symp. Interactive 3D Graphics*, 149-154, 1997.

[7] S. F. F. Gibson, Using linked volumes to model object collisions, deformation, cutting, carving, and jointing, *IEEE Trans. on Visual. & comp. Graph.,* **5**, 333-348, 1999.

[8] Y. Wang, H. N. Cardinal, D. B. Downey, and A. Fenster, Semiautomatic three-dimensional segmentation of the prostate using two-dimensional ultrasound images, *Med Phys*, **30**, 887-897, 2003.

[9] M. A. Schill S. F. F. Gibson, H. –J. Bender, and R. Manner, Biomechanical simulation of the vitreous humor in the sys using an enhanced ChainMail algorithm, *Medical Image Computing and Computer Assisted Intervention* (*MICCAI'* 1998), 679-687.

[10] W. M. Hsu, J. F. Hughes and H. Kaufman, Direct manipulation of free-form deformation, in *Computer Graphics* (*proc*. SIGGRAPH), 177-182, 1992.

[11] C. Simone and A. M. Okamura, Modeling of the needle insertion forces for robot-assisted percutaneous therapy, in *Proc. of the IEEE Int. Conf. on Robotics and Auto.*, May, 2085-2091, 2002.

[12] J. B. Ra, S. M. Kwon, J. K. Kim, and et. al., Spine needle biopsy simulator using visual and force feedback, *Computer Aided Surgery*, **6**, 353-363, 2002.

[13] X. Wang and A. Fenster, A haptic-enhanced 3D real-time interactive needle insertion simulation system for prostate brachytherapy, to appear in *Proc. of the SPIE Medical Imaging,* Feb., 2004.